

The Effect of Common-Mode Voltage Elimination on the Iron Loss in Machine Core Laminations of Multilevel Drives

A. Salem^{1,2}, A. Abdallah^{1,3}, P. Rasilo⁴, F. De Belie¹, M. N. Ibrahim¹, L. Dupré¹, and J. Melkebeek¹

¹Department of Electrical Energy, Systems & Automation, Ghent University, Belgium

²Electrical Power & Machines Department, Helwan University, Egypt

³Electrical Power & Machines Department, Cairo University, Egypt

⁴Department of Electrical Engineering & Automation, Aalto University, Finland

Abstract—This paper studies the effect of common-mode voltage elimination (CMVE) on the iron loss of electrical machine core laminations under multilevel converter supply. Three identical magnetic ring cores are excited by either a three-level converter or a five-level voltage source converter to study the behavior of CMVE on a three-phase system. Both multilevel converters are controlled by using a space vector pulse width modulation as it is one of the most often used techniques for CMVE. These experimental results are confirmed numerically with a dynamic iron loss model. In addition, the effect of CMVE, at different switching frequencies, on the core loss of a synchronous machine is numerically studied. The results presented in this paper show that the core loss is considerably increased when the CMVE is implemented. However this iron loss increase in five-level drive systems is lower compared to the three-level ones. Therefore, it is important that the designers of drive systems take such effects into consideration.

Index Terms—Common-mode voltage elimination, iron loss, magnetic material, multilevel converters, pulse width modulation.

I. INTRODUCTION

THE voltage source multilevel converter has become an essential part of modern electrical ac drives. Its main function is to generate a three-phase supply voltage at a given desired frequency. However it generates also a common mode voltage (CMV) at a relatively high frequency. This voltage has a dramatic effect on the machine bearings and insulations. Moreover, it causes an electromagnetic interference which has undesirable effects on the digital controller and the equipped sensing units [1]. A frequently used modulation technique to eliminate the CMV in multilevel converters is the space vector pulse width modulation (SVPWM). The CMV elimination (CMVE) using the SVPWM is based on modifying the switching scheme of the converter switches in order to deliver a zero third harmonic content, and its multiples, in the converter phase voltage [1]. The use of some space voltage vectors is omitted, in particular those that contribute to the generation of a third harmonic content in the converter phase voltage. Although CMVE enhances the performance of the drive, in terms of the bearing lifetime, it is also expected to affect the iron loss of the machine, and consequently the machine efficiency.

Although the effect of the PWM on the iron loss has been extensively studied up to this date [2], [3], to the best of the authors' knowledge, the effect of CMVE on the iron loss of electrical machines has not been fully described in details. A theoretical analysis to evaluate the increase of the motor PWM loss due to CMVE for a conventional three-level converter was given in [4]; however, neither iron loss measurements nor computational verifications were performed.

In the work presented here, the three-level (dual two-level topology) converter, as well as the five-level (dual T-type topology) converter, are studied using the SVPWM technique in the unmodified modulation case as well as in the CMVE case. The converters are experimentally tested on three identical magnetic ring cores as a three-phase load to show the effect of the CMVE on the iron loss of non-oriented electrical steel. Moreover, the effect of the CMVE on the core loss of a synchronous machine is numerically analyzed. Both studies are performed at different switching frequencies to clarify the effect of the frequency on the iron loss.

This paper is organized as follows. Section II describes the used experimental setup. The converter circuits are given followed by a brief description of the CMV phenomenon and the CMVE principle. In addition, the iron loss measurement on the ring core is discussed. In section III, the numerical technique, including the dynamic iron loss model, is shortly outlined. Afterwards, in section IV, the experimental and the simulation results are presented and discussed. Finally, the conclusions are drawn in section V.

II. EXPERIMENTAL SETUP

The used experimental setup is flexible to supply a three-phase load with different multi-level converter topologies. The three-level as well as the five-level voltage source converters are tested and analyzed with three identical magnetic ring cores, to emulate a three-phase system, as shown in Fig. 1. A SVPWM technique, which is implemented on a field programmable gate array (FPGA) digital controller, is used to generate the output voltage in two considered case studies, i.e. without CMVE (unmodified case) and with CMVE.

The converter circuits, the CMV generation and the procedure of the iron loss measurements are presented in the following subsections.

A. Converter circuits

The circuit configuration used for both converter types is shown in Fig. 1. In Fig. 2, the two types of converters (three-level and five-level respectively) are depicted. Here, discrete power electronic metal oxide field effect transistors, with a code number of IXKR-40N60C, are utilized. When the SVPWM is applied to the converters, the possible operating vectors can be represented by the vector diagram, which is referred to as *hexagon* as shown in Fig. 3. The solid and dashed

This work is supported by Erasmus Mundus Action-2 WELCOME Program, the Special Research Fund (BOF) of Ghent University, the project (IAP-VII-02), and the Academy of Finland. Corresponding author: A. A-E. Abdallah (e-mail: ahmed.abdallah@ieee.org).

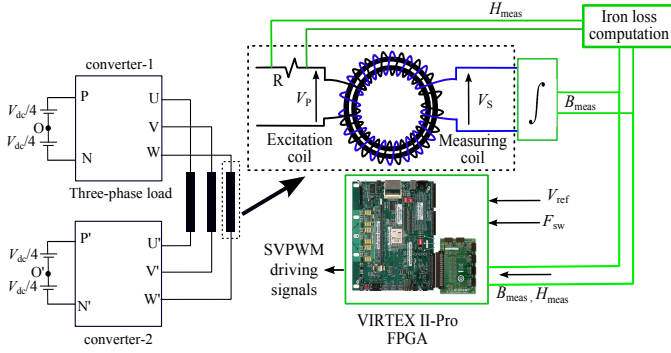


Fig. 1. Block diagram for the operating system.

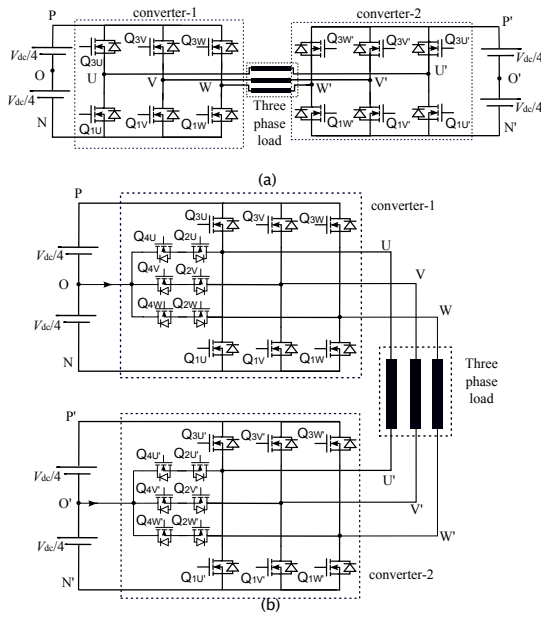


Fig. 2. Schematic diagram of the three-phase circuit of (a) three-level converter, (b) five-level converter circuits connected to a three-phase load.

line hexagons represent the unmodified and CMVE operating conditions, respectively. In the unmodified operating condition, there are 19 and 61 possible vectors for the three and five-level converters, respectively.

B. CMV phenomenon and its elimination principle

CMV naturally appears in ac drives that use voltage source converters. Generally speaking, CMV is defined as the instantaneous voltage difference between the two grounds of two isolated power systems [1]. In the used converter circuits, the CMV of converter-1 (v_{CMV1}), the CMV of converter-2 (v_{CMV2}) and the CMV of the dual converter configuration can be expressed by (1-3).

$$v_{CMV1} = \frac{1}{3}(v_{UO} + v_{VO} + v_{WO}), \quad (1)$$

$$v_{CMV2} = \frac{1}{3}(v_{U'O'} + v_{V'O'} + v_{W'O'}), \quad (2)$$

$$v_{CMV} = v_{CMV1} - v_{CMV2}. \quad (3)$$

This voltage has a considerable third harmonic and its multiples [1], see later in section IV. In order to eliminate the CMV

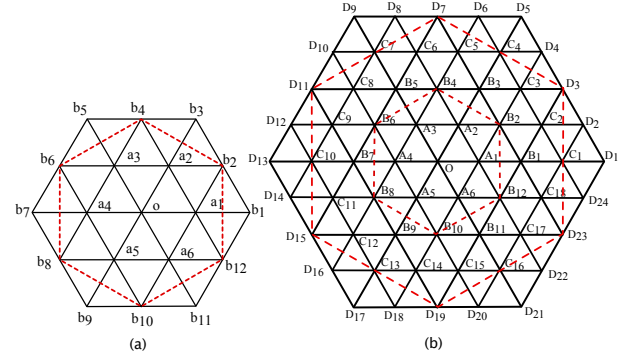


Fig. 3. Vector diagram (hexagon) for (a) three-level converter, and (b) five-level converter. Solid and dashed lines are for unmodified and CMVE case studies, respectively.

from a drive-system, it is essential to analyze the converter operating space vector and classify it into two groups, i.e. effective vectors which deliver a CMV and ineffective vectors which result in a zero CMV. By analyzing the switching possibilities for each converter, the ineffective vectors can be represented by the *hexagon*, shown in dash-lines in Fig. 3. Specifically, when the CMV needs to be mitigated, the vectors on the dashed line hexagon are only used. In the CMVE operating condition, there are only 7 and 13 out of 19 and 61 possible vectors of the three and five-level converters, respectively. For more information about the CMVE, see [5].

C. Iron loss measurement of the magnetic ring core

Three identical uniformly wound magnetic ring cores, each with two windings; excitation and measurement windings, are designed to form a balanced three-phase load supplied from both ends as shown in Fig. 1. The magnetic core properties, i.e. the magnetic field strength (H) and magnetic flux density (B), are obtained using the field-metric technique. The magnetic ring cores are constructed from 0.5 mm non-oriented electrical steel sheets using the spark erosion cutting technique. Each core is composed of 20 laminations with 90 mm and 110 mm, internal and external diameters, respectively.

For the sake of comparison, the measurements are performed so as to achieve a sinusoidal magnetic induction waveform in the magnetic core. To this end, the converter is iteratively feed-back controlled in order to deliver a prescribed fundamental component of the magnetic induction (with a maximum deviation of 0.05%). A wide range of magnetic inductions, from the demagnetized state up to saturation, is tested. Additionally, the test is performed at different switching frequency values, i.e. at 1, 2.5, 5 and 10 kHz, in order to study the switching frequency effect on the iron loss in the two aforementioned case studies. The iron loss P is calculated for each magnetic induction waveform by integrating the measured B - H hysteresis loop:

$$P = \frac{f}{\gamma} \cdot \oint H(B)dB \quad (4)$$

where P , f and γ are the iron loss per unit mass, in (W/kg), the fundamental power frequency, in (Hz), and the mass density of the electrical steel, i.e. $\gamma = 7650 \text{ kg/m}^3$.

III. NUMERICAL ANALYSIS

A. Dynamic iron loss model

The iron losses are numerically modeled with the approach described in detail in [6]. The flux density in the thickness $z \in [-d/2, d/2]$ of one lamination is expressed as a cosine series:

$$\mathbf{b}(z, t) = \sum_{n=0}^{N_b-1} \mathbf{b}_n(t) \alpha_n(z), \text{ with } \alpha_n(z) = \cos\left(2\pi n \frac{z}{d}\right). \quad (5)$$

When the average flux density $\mathbf{b}_0(t)$ in the lamination is known, the field strength $\mathbf{h}_s(t)$ on the lamination surface as well as the higher-order terms $\mathbf{b}_n(t)$ can be solved from

$$\begin{bmatrix} \mathbf{h}_s(t) \\ 0 \\ \vdots \end{bmatrix} = \frac{1}{d} \int_{-d/2}^{d/2} \mathbf{h}(\mathbf{b}(z, t)) \begin{bmatrix} \alpha_0(z) \\ \alpha_1(z) \\ \vdots \end{bmatrix} dz + \sigma d^2 \mathbf{C} \begin{bmatrix} \mathbf{b}'_0(t) \\ \mathbf{b}'_1(t) \\ \vdots \end{bmatrix}, \quad (6)$$

in which σ is the conductivity of the lamination and \mathbf{C} is a constant matrix. The local $\mathbf{h}(\mathbf{b}(z, t))$ relationship consists of a static vector Preisach hysteresis model and a dynamic contribution corresponding to the excess losses. After the flux-density distribution (5) is known, the classical eddy-current, hysteresis and excess losses can be calculated in a straightforward way and averaged over the lamination thickness.

B. Finite element machine model

In order to study the effect of CMVE in an electrical machine, a 150 kVA, 400 V, 50 Hz, 4-pole synchronous generator is modeled with a time-stepping finite element (FE) method. Fig. 4 shows the 2-D cross-sectional FE mesh of the machine. The iron-loss model (5)-(6) is implemented in the laminated regions using a magnetic vector potential formulation [6]. The stator winding is supplied by SVPWM voltage waveform including a 230 V fundamental voltage component, while a dc voltage is supplied in the field winding and the rotor rotates with constant speed. The total core losses consist of the hysteresis, classical eddy current and excess losses, damper winding losses as well as eddy-current losses in the stator frame. It is worth noting that in other control schemes, such as direct torque control, a coupled simulation model of the converter and the machine over multiple periods could be required in order to take into account the stochastic switching pattern [7], [8].

IV. RESULTS AND DISCUSSION

A. Ring core

By applying the aforementioned converter circuits to the ring core coils, the phase voltage in the unmodified and CMVE cases, as well as the CMV itself at $F_{sw} = 5$ kHz are shown in Fig. 5 for the five-level converter at 1.5 T. It is clear from this figure that the CMV has a third harmonic component which would affect the bearing life-time in an electrical machine. Notice that neither in the unmodified case nor in the CMVE case, the phase voltage will contain that third harmonic. Similar results are obtained in the three-level converter.

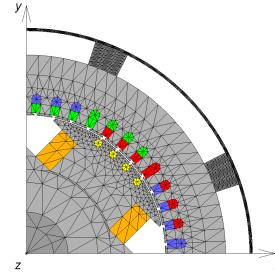


Fig. 4. Geometry and the FE mesh of the studied machine.

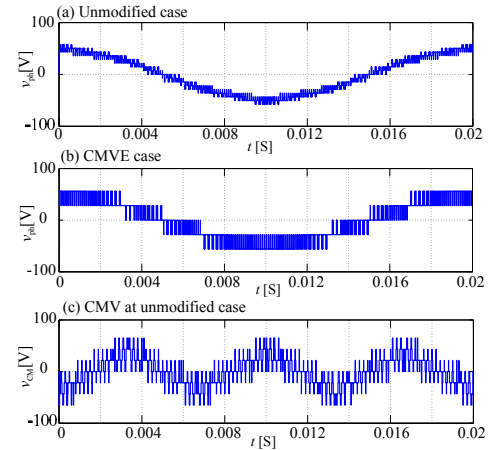


Fig. 5. Phase voltage in (a) the unmodified case, (b) the CMVE case. (c) The CMV for the five-level converter at 1.5 T and 5 kHz switching frequency.

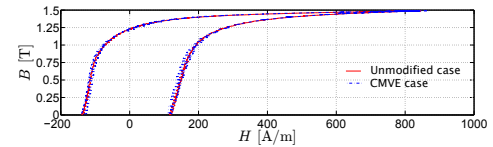


Fig. 6. The half of the measured B - H hysteresis loop for the five-level converter at 1.5 T.

Fig. 6 shows the measured hysteresis loop for the five-level converter at $F_{sw} = 5$ kHz and 1.5 T. More minor loops are noticeable in the CMVE case, which increase the iron loss. A similar trend is also noted for the three-level converter. Fig. 7 shows the iron loss at different values of induction level in all case studies, at $F_{sw} = 5$ kHz. The effect of CMVE is negligible at low induction values.

Fig. 8 depicts the measured and simulated iron loss of the magnetic core at $F_{sw} = 1, 2.5, 5$ and 10 kHz and at 1.5 T. Compared to the unmodified case, the CMVE case increases the iron loss, e.g. on average by almost 3% and 1%, for three-level and five-level converters, respectively. A similar trend is observed numerically using the dynamic iron loss model presented in section III, which supports the experimental results. The experimental results also reveal the superiority of the higher converter levels over the lower levels. In principle, the five-level converter does not only result in a lower iron loss compared to the three-level converter, as was outlined in [9], but also results in a lower rate of rise of the iron loss due to the CMVE.

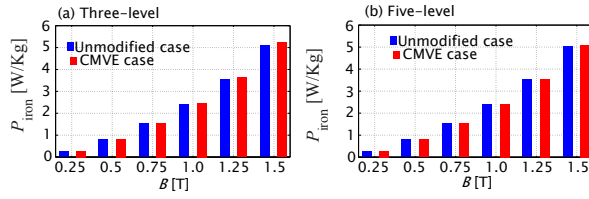


Fig. 7. Measured iron loss in the ring core in the unmodified and CMVE cases, in (a) three-level and (b) five-level converter at different magnetic inductions and at $F_{sw} = 5$ kHz.

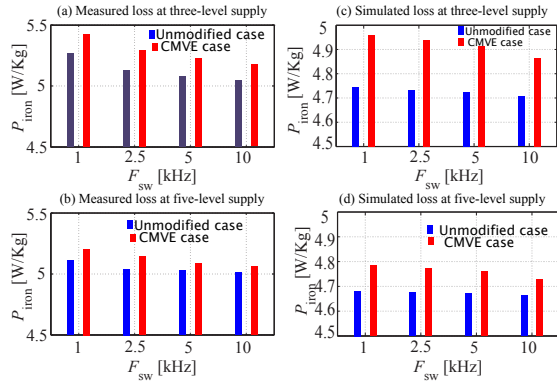


Fig. 8. Measured iron loss in the (a) three-level and (b) five-level drive systems. Simulated iron loss in the (c) three-level and (d) five-level drive systems. All results at 1.5 T and at different switching frequencies.

B. Machine core loss

This section discusses the simulation results for the synchronous machine. The machine is tested using the aforementioned converter circuits at different switching frequencies and different loading conditions, i.e. half and full-load. The converters are controlled by means of the SVPWM technique for both unmodified and CMVE case studies.

Fig. 9 shows the machine core loss at half and full-load operation conditions and at different switching frequencies. From that figure it follows that the CMVE increases the core loss with 10%-20% for a three-level converter and 5%-10% for a five-level converter. Moreover, they endorse the experimental results on the magnetic ring core. Increase in core loss due to the application of CMVE is the largest for a three-level converter. However, the higher the switching frequency, the smaller this increase in core loss due to CMVE becomes. For example, at full load operation conditions, the core loss increases by almost 15 % to 8 % when the F_{sw} varies from 1 to 10 kHz in three-level converter, and by almost 6 % to 4% in the five-level converter. It is worth noting that the core loss for the three-level supply in the unmodified case is quite close to the core loss values in the five-level supply for the CMVE case. Hence, the authors recommend to use higher level converters when the CMV needs to be effectively mitigated. Moreover, future research on electrical machine needs to consider the effect of CMVE for a better performance of the complete drive system.

V. CONCLUSION

This study investigated the effect of CMVE of multilevel converter drive systems on the iron loss within machine core

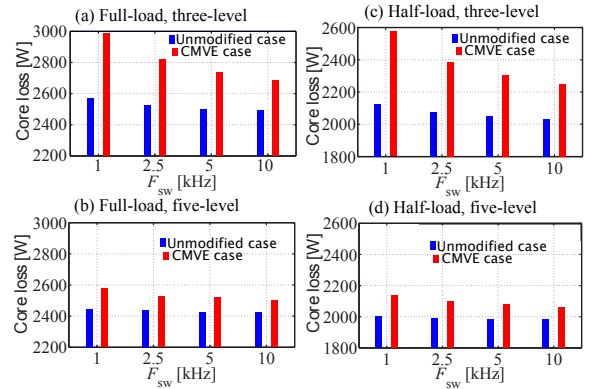


Fig. 9. Simulated core loss in the synchronous machine at the full load operation condition for (a) the three-level and (b) the five-level converter supply. The losses at half load operation condition for (c) the three-level and (d) the five-level converter supply.

laminations. First, magnetic measurements were carried out on a magnetic ring core to investigate the iron loss in both three and five level converters. Experiments were conducted at different switching frequencies. The experimental work was verified numerically using a dynamic iron loss model. Then, the dynamic iron loss model was coupled with a finite element model of a synchronous machine to calculate the effect of the CMVE on the synchronous machine core loss at different loading conditions. Results on both the magnetic ring core as well as the synchronous machine reflect the bad effect of the CMVE on the iron loss. Although the CMVE improves the bearing life time, it deteriorates the efficiency of the drive system. Moreover, a higher multilevel converter topology showed a better performance than converters with a smaller number of voltage levels.

REFERENCES

- [1] J. Kalaiselvi, K. Rama, and S. Srinivas, "Common mode voltage elimination PWMs for a dual two-level VSI with single inverter switching," *IEEE International Symposium on Industrial Electronics (ISIE)*, pp. 234 - 239, 2012.
- [2] T. Sasayama, M. Morita, and M. Nakano, "Experimental Study on Effect of Load on Iron Loss of an Electrical Steel Sheet Under PWM Inverter Excitation," *IEEE Trans. Magn.*, vol. 50, no. 11, Art. no. 6000504, 2014.
- [3] M. Merdzan, A. Borisavljevic, E. A. Lomonova, "Modeling the influence of commutation in voltage source inverters on rotor losses of permanent magnet machines," *16th European Conference on Power Electronics and Applications (EPE'14-ECCE Europe)*, pp. 1-10, 2014.
- [4] A. Ruderman and B. Reznikov, "Evaluation of motor PWM loss increase due to zero common-mode voltage modulation strategy of multilevel converter," *Power Electronics and Motion Control Conference (EPE/PEMC)*, pp. 66-72, 2010.
- [5] B. Yang, W. Li, Y. Gu, W. Cui, and X. He, "Improved transformerless inverter with common-mode leakage current elimination for a photovoltaic grid-connected power system," *IEEE Trans. Power Electron.*, vol. 27, no. 2, pp. 752-762, 2012.
- [6] P. Rasilo, A. Belahcen, and A. Arkkio, "Importance of iron-loss modeling in simulation of wound-field synchronous machines," *IEEE Trans. Magn.*, vol. 48, no. 9, pp. 2495-2504, 2012.
- [7] S. Kanerva, J. Kaukonen, A. Szucs, T. Hautamaki, "Coupled FEM-Control Simulation in the Analysis of Electrical Machines and Converters," *Power Electronics and Motion Control Conference (EPE/PEMC)*, pp. 1925-1930, 2006.
- [8] K. Satyanarayana, P. Surekha, and P. Vijaya Prasuna, "A DTC based FOC Strategy of Induction Motor drive for the Mitigations of CMV," *Acta Electrotechnica*, vol. 54, no. 3-4, pp. 190-196, 2013.
- [9] A. Salem, A. Abdallah, F. De Belie, L. Dupré, and J. Melkebeek, "A comparative analysis of the effect of different converter topologies on the iron loss of nonoriented electrical steel," *IEEE Trans. Magn.*, vol. 50, no. 11, Art. no. 6000804, 2014.